Computational smoldering combustion: Predicting the roles of moisture and inert contents in peat wildfires

Xinyan Huang [a], Guillermo Rein [a,*], Haixiang Chen [b]

[a] *Department of Mechanical Engineering, Imperial College London, UK*
[b] *State Key Laboratory of Fire Science, University of Science and Technology of China, Hefei 230026, Anhui, China*

Available online 25 June 2014

Abstract

Smoldering combustion is the slow, low-temperature, flameless burning of porous fuels and the most persistent type of combustion. It is the driving phenomenon of wildfires in peatlands, like those causing haze episodes in Southeast Asia and Northeast Europe, but is poorly understood. In this work, we develop a comprehensive 1-D model of a reactive porous media, using the open-source code Gpyro, to investigate smoldering combustion of natural fuels with an emphasis on the roles of the moisture and inert contents. The model solves the species, momentum, and energy conservation equations and includes heterogeneous chemical reactions. A previously developed 5-step reaction scheme for peat, including evaporation of water, is adopted to describe the drying, thermal and oxidative degradation during the smoldering combustion. The model predicts the transient temperature, species, and reaction profiles during ignition, spread, and extinction. The predicted smoldering thresholds related to the critical moisture and inorganic contents for ignition show a good agreement with the experimental results in the literature for a wide range of peat types and organic soils. The influences of the kinetic parameters, physical properties, and ignition protocol are investigated. This is the first time that a physics-based model of smoldering peat fires is developed, thus helping to understand this important natural and widespread phenomenon.
© 2014 The Authors. Published by Elsevier Inc. on behalf of The Combustion Institute. This is an open access article under the CC BY license (http://creativecommons.org/licenses/by/3.0/).

Keywords: Peat wildfires; Smoldering combustion; Computational; Drying; Smoldering thresholds

1. Introduction

Smoldering combustion is the slow, low-temperature, flameless burning of porous fuels and the most persistent type of combustion [1]. Smoldering is the dominant phenomenon in megafires in natural deposits of peat which are the largest and longest burning fires on Earth. These fires contribute considerably to global greenhouse gas emissions, and result in widespread destruction of ecosystems and regional haze events (e.g. recent megafires in Southeast Asia, North America and Northeast Europe) [2]. It is an emerging research topic in climate change mitigation but is poorly understood. For example, during the 1997 extreme haze event in Southeast Asia, peat fires emitted the equivalent to 13–40% of the global man-made greenhouse gas emissions of that year [3]. Rein [2] has pointed out that the atmospheric release of ancient carbon from the soil and the

---

* Corresponding author. Fax: +44 (0)20 7594 7036.
 E-mail address: G.Rein@imperial.ac.uk (G. Rein).

Nomenclature

A	pre-exponential factor
c_p	heat capacity
d_p	characteristic pore size
C	heat of complete oxidation
E	activation energy
h	enthalpy
h_c	convective coefficient
h_m	mass-transfer coefficient
k	thermal conductivity
K	permeability
$\dot{m}''$	mass flux
n	heterogeneous reaction order
P	pressure
R/R_s	universal/specific gas constant
S	particle surface area
t	time
T	temperature
Y	mass fraction
z	distance
IC/MC	inorganic/moisture content

Greeks

γ	radiative conductivity coefficient
ε	emissivity
v	viscosity/stoichiometric coefficient
ρ	bulk density (mass concentration)
ρ_s	solid density, $\rho/\rho_s = 1 - \psi$
σ	Stefan–Boltzmann constant
χ	fraction factor
ψ	porosity
$\dot{\omega}$	reaction rate

Subscripts

0	initial
$\alpha/\alpha o$	α-char/α-char oxidation
$\beta/\beta o$	β-char/β-char oxidation
a	ash
d/f	destruction/formation
dr	drying
g	gas
i	condensed species number
j	gaseous species number
k	reaction number
$p/po/pp$	peat/peat oxidation/peat pyrolysis
w	water

sensitivity of peat ignition to higher temperatures and drier soils could create a positive feedback mechanism for climate change.

Peat can hold a wide range of moisture contents (MC[1]), ranging from 10%, under drought conditions, to in excess of 300%, under flooded conditions [4]. Water represents a significant energy sink, and furthermore natural or anthropogenic-induced droughts are found to be the leading cause of smoldering megafires [5,2]. Therefore, soil moisture is the single most important property governing the ignition and spread of smoldering wildfires [5–7]. The critical moisture content (MC$_c$) for initiating smoldering of various boreal peat has been measured in the range 40–150% in dry basis [7,8]. Drier than this threshold, peat becomes susceptible to smoldering. The second most important property is the soil inorganic content (IC[1]). As experimentally found by Frandsen [6,7], there is a decreasing quasi-linear relationship between MC$_c$ and IC$_c$: soil with a high IC can only be ignited at low MC. Mineral matter acts as a heat sink but also enhances the heat transfer via its higher heat conductivity. After moisture and inorganic contents, other important properties are bulk density, porosity, flow permeability and organic composition [2].

The spread of smoldering fires is controlled by heat and mass transfer processes in a reactive porous media. The computational studies on smoldering combustion in the literature have only included three fuels: cellulose [1,9], polyurethane foam [1,8] and char [10], simulated with chemical schemes of different complexity, including 1 [10], 3 [1] or 5 [8] steps. Ohlemiller [1] reviewed the early attempts on simulating smoldering combustion and provided the governing equations in general form. Rein et al. [8] numerically solved the 1-D smoldering combustion of polyurethane foam under forced flow with a 5-step kinetics, and the results were compared to microgravity experiments in both opposed and forward propagation modes. He et al. [10] developed a 1-D model to solve the in-depth spread of smoldering for char with 1-step chemistry and compared it to the experiments. Previous studies have not considered simulations of peat fires or the drying process.

In this work, we use a comprehensive 1-D model based on Gpyro [11] and a previously developed 5-step kinetics (including drying) for peat kinetics [12] to investigate the ignition and spread of smoldering in a bed of peat and other organic soils. Prediction of the smoldering

---

[1] Moisture content (MC) is defined in dry basis as the mass of water divided by the mass of a dried soil sample, expressed as %. Inorganic content (IC < 100%) is defined in dry basis as the mass of soil inorganic matter (minerals) divided by the mass of a dried soil sample, expressed as %.

thresholds related to MC_c and IC_c are the emphasis. The computational results are compared with experiments [6,7]. The influences of the kinetic parameters, ignition protocol, and physical properties are investigated.

2. Computational model

Frandsen [6,7] conducted two sets of pioneer experiments to determine the smoldering thresholds of multiple soil samples. In the first set of experiments [6], natural peat moss of negligible minerals (IC = 3.7%) was mixed with water (m_w) and mineral clay (m_{cl}) to produce modified soil samples of known $MC = m_w/(m_p + m_{cl})$ and $IC = m_{cl}/(m_p + m_{cl})$. The modified samples were tested in an insulated box with the top open to the atmosphere, of a depth of 40 mm and a cross section of 90×90 mm (internal dimension). A coil heater was in contact with the top surface for 3 min to initiate the smoldering at least near the coil. In the second set of experiments [7], a large number of unmodified natural soil samples with different natural ICs at various sites of North America were tested to find MC_c and IC_c. The ignition protocol was different: an additional layer of dry peat of 10 mm was placed between the coil heater and the soil sample.

During smoldering, the peat is first dried and decomposed to char, and then char is oxidized to ash [2,12]. After the ignition of a vertical sample, a smoldering front starts to spread in-depth and a layer of ash is accumulated on the top, as illustrated in Fig. 1. Depending on both MC and IC, this smoldering front may become self-sustaining and consume most of the organic matter, or may not spread beyond the ignition zone. As a first approximation, Frandsen's experiments can be modelled as 1-D at the in-depth direction
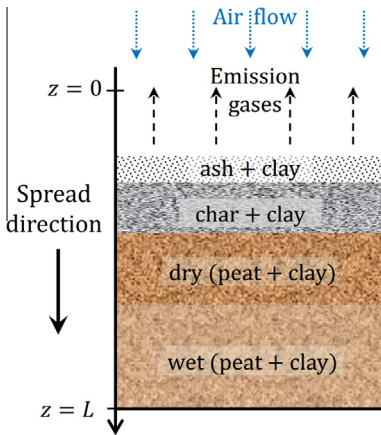
because buoyancy plays a negligible role in these relatively small samples (40 mm), i.e. vertical and horizontal samples behave the same way. We used the open-source code Gpyro [11] to implement a 1-D model and simulate the ignition and spread of smoldering combustion of peat.

2.1. 1-D governing equations

The computational domain is a 40 mm deep sample with ignition at the top free surface and insulated at the bottom (Fig. 1). The model solves the 1-D transient equations for both solid and gas phases in the absence of gravity. The gas-phase temperature is assumed to be the same as the condensed-phase temperature (thermal equilibrium). The details are reported in [11]; only the essential conservation equations are presented here: (1) condensed-phase mass, (2) condensed-phase species, (3) condensed-phase energy, (4) gas-phase mass, (5) gas-phase species, and (6) gas-phase momentum (Darcy's law). Symbols are explained in the nomenclature, and subscripts $i, j,$ and k refer to the number of condensed-phase species, gas-phase species, and reaction, respectively.

$$\frac{\partial \overline{\rho}}{\partial t} = -\dot{\omega}_{fg}''' \tag{1}$$

$$\frac{\partial (\overline{\rho} Y_i)}{\partial t} = \dot{\omega}_{fi}''' - \dot{\omega}_{di}''' \tag{2}$$

$$\frac{\partial (\overline{\rho} h)}{\partial t} = \frac{\partial}{\partial z}\left(\overline{k}\frac{\partial T}{\partial z}\right) + \sum_{k=1}^{K} \dot{Q}_{s,k}''' + \left(\dot{\omega}_{fi}''' - \dot{\omega}_{di}'''\right)h_i \tag{3}$$

$$\frac{\partial (\rho_g \overline{\psi})}{\partial t} + \frac{\partial \dot{m}''}{\partial z} = \dot{\omega}_{fg}''' \tag{4}$$

$$\frac{\partial (\rho_g \overline{\psi} Y_i)}{\partial t} + \frac{\partial (\dot{m}'' Y_j)}{\partial z} = -\frac{\partial}{\partial z}\left(\overline{\psi}\rho_g D \frac{\partial Y_j}{\partial z}\right) + \dot{\omega}_{fj}''' - \dot{\omega}_{dj}''' \tag{5}$$

$$\dot{m}'' = -\frac{\overline{K}}{v}\frac{\partial P}{\partial z} \qquad (P = \rho_g R_s T) \tag{6}$$

Each condensed-phase species is assumed to have constant properties (e.g. bulk density, specific heat, and porosity). All gaseous species have unit Schmidt number, and equal diffusion coefficient and specific heat. The averaged properties in each cell are calculated by weighting appropriate mass or volume fractions [11].

At the free surface ($z = 0$), the convective boundary condition is imposed $h_{c,o} = 10$ W/m²·K with reradiation ($\varepsilon = 0.95$) and mass transfer $h_{m,0} = 0.02$ kg/m² · s (approximation of Couette flow [11]). The ambient pressure and temperature are assumed to be atmospheric and 300 K. Within the first 3 min, a heat flux of 30 kW/m² is applied to simulate the heating of the coil heater (the effect of the heat flux level is explored in Section 4.2). At the deep end of the sample ($L = 40$ mm), the mass flux is set to zero, and heat loss is set with $h_{c,L} = 3$ W/m² · K. A fully implicit formulation is

Fig. 1. Illustration of the 1-D computational domain for in-depth spread of smoldering in a sample of peat.

adopted for solution of all equations. More details about the numerical solution are reported in [11]. Simulations were run with an initial cell size of $\Delta z = 0.1$ mm (400 cells per domain), and an initial time step of 0.01 s. Reducing the cell size and time step by a factor of 2 gives no significant difference in results, so the calculations are sufficiently resolved.

2.2. Chemical kinetics

The heterogeneous reaction in mass basis is written as:

$$A_k + \sum_{j=1}^{N} v'_{j,k}\text{gas } j \rightarrow v_{B,k}B_k + \sum_{j=1}^{N} v''_{j,k}\text{gas } j, \quad (7)$$
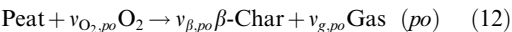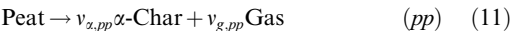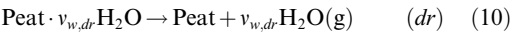
where $v_{B,k} = 1 + (\rho_B/\rho_A - 1)\chi_k$, and χ_k quantifies the shrinkage or intumescence of the cell size. The destruction rate of condensed species A in reaction k is expressed by the Arrhenius law

$$\dot{\omega}'''_{dA_k} = \frac{(\overline{\rho}Y_A\Delta z)_{\Sigma}}{\Delta z} Z_k e^{-E_k/RT} \left[\frac{\overline{\rho}Y_A\Delta z}{(\overline{\rho}Y_A\Delta z)_{\Sigma}}\right]^{n_k} Y_{O_2}^{n_{O_2,k}}, \quad (8)$$

$$(\overline{\rho}Y_A\Delta z)_{\Sigma} = (\overline{\rho}Y_A\Delta z)|_{t=0} + \int_0^t \dot{\omega}'''_{fi}\Delta z(\tau)d\tau, \quad (9)$$

where subscripts d and f represent destruction and formation. The formation rate of condensed species B and all gases from reaction k are $\dot{\omega}'''_{fB_k} = v_{B,k}\dot{\omega}'''_{dA_k}$ and $\dot{\omega}'''_{fg_k} = (1 - v_{B,k})\dot{\omega}'''_{dA_k}$. The corresponding heat of reaction is $\dot{Q}'''_k = -\dot{\omega}'''_{dA_k}\Delta H_k$.

In previous work [12] the decomposition schemes with different complexities were investigated using thermogravity (TG) data of four different peat samples from Scotland (SC), Siberia (SI-A and SI-B), and China (CH). The best kinetics scheme was found to be: (1) drying (dr), (2) peat pyrolysis (pp), (3) peat oxidation (po), (4) β-char oxidation (βo), and (5) α-char oxidation (αo) as

$$\text{Peat} \cdot v_{w,dr}H_2O \rightarrow \text{Peat} + v_{w,dr}H_2O(g) \quad (dr) \quad (10)$$

$$\text{Peat} \rightarrow v_{\alpha,pp}\alpha\text{-Char} + v_{g,pp}\text{Gas} \quad (pp) \quad (11)$$

$$\text{Peat} + v_{O_2,po}O_2 \rightarrow v_{\beta,po}\beta\text{-Char} + v_{g,po}\text{Gas} \quad (po) \quad (12)$$

$$\beta\text{-Char} + v_{O_2,\beta o}O_2 \rightarrow v_{a,\beta o}\text{Ash} + v_{g,\beta o}\text{Gas} \quad (\beta o) \quad (13)$$

$$\alpha\text{-Char} + v_{O_2,co}O_2 \rightarrow v_{a,\alpha o}\text{Ash} + v_{g,\alpha o}\text{Gas} \quad (\alpha o) \quad (14)$$

where subscripts w, p, α, β, and a represent five condensed species (water, peat, α-char, β-char, and ash), in addition to four gaseous species: oxygen, nitrogen, water vapour, and emission gases.

3. Smoldering structure

3.1. Parameter selection

The physical properties of the condensed-phase species are listed in Table 1. The solid ($\psi = 0$) physical properties, $\rho_{s,i}, k_{s,i}, c_{p,i}$ of peat, char, and clay are selected from [13]. The porosity

Table 1
The physical parameters of condensed-phase species before mixing where $\rho_{s,i}, k_{s,i}$, and $c_{p,i}$ are from [13], and $\rho_{i,0}$ is from [6,16].

Species (i)	$\rho_{s,i}$ (kg/m³)	$\rho_{i,0}$ (kg/m³)	$\psi_{i,0}$ (−)	$k_{s,i}$ (W/m·K)	$c_{p,i}$ (J/kg·K)
Water	1000	1000	–	0.6	4186
Peat	1500	110	0.927	1.0	1840
α-Char	1300	135	0.896	0.26	1260
β-Char	1300	135	0.896	0.26	1260
Ash	2500	19.5	0.992	0.8	880
Clay	2500	1200	0.520	0.8	880

is calculated using the bulk density in the literature as $\psi_i = (1 - \rho_i/\rho_{s,i})$. The effective thermal conductivity includes the radiation heat transfer across pores as $k_i = k_{s,i}(1 - \psi_i) + \gamma\sigma T^3$ where $\gamma = 10^{-4} \sim 10^{-3}$ m depends on the pore size ($\gamma \sim d_p = 1/S\rho$) with a soil particle surface area $S \sim 0.05$ m²/g [14]. The permeability ($K \sim d_p^2$) varies from 10^{-12} to 10^{-9} m² [15].

The sample volume expands after peat is mixed with clay, but for unsaturated samples, water occupies the pore space and does not expand the volume. Thus, the bulk density of mixed unsaturated soil is given as $\rho = (1 + MC)/[(1 - IC)/\rho_p + IC/\rho_{cl}]$. The properties of α-char and β-char are assumed to be the same, and so as natural minerals (ash) and clay. After combustion, the residue is a homogenous mixture of natural minerals and clay.

The Scotland (SC) peat sample with a high organic content (IC = 1.8%) [12] is selected as the base case. Table 2 lists the kinetic and stoichiometric parameters. The heat of oxidation is related to the fraction of oxidized organic matter and assumed to be $\Delta H_k = C_k(1 - v_k)$. By integrating the energy–flux curve of TG-DSC measurements of multiple peat samples [17,18], $C_{po} = 10$ MJ/kg and $C_{\alpha o} = C_{\beta o} = 20$ MJ/kg are selected. Under TG conditions and a sufficient air supply, the total heat of combustion for a dry SC samples is calculated to be 15 MJ/kg, similar to measured values in [17,19]. We relate the oxygen consumption to the heat of oxidation by assuming a constant heat of combustion per unit of oxygen consumed as $v_{O_2,k} = \Delta H_k/(13.1$ MJ/kg) [20].

Table 2
Reaction parameters and gaseous yields of 5-step reactions for SC peat sample [12].

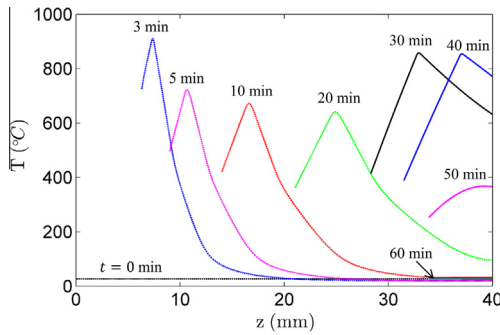| Parameter/k	dr	pp	po	αo	βo
$\lg A_k$ (lg(s^{-1}))	8.12	5.92	6.51	1.65	7.04
E_k (kJ/mol)	67.8	93.3	89.8	54.4	112
n_k (−)	2.37	1.01	1.03	0.54	1.85
$v_{B,k}$ (kg/kg)	0	0.75	0.65	0.03	0.02
ΔH_k (MJ/kg)	2.26	0.5	−3.54	−19.5	−19.5
$v_{O_2,k}$ (kg/kg)	0	0	0.27	1.48	1.49

Fig. 2. Predicted evolution of the temperature profile at different depths for SC peat with MC = 30% and IC = 40%.

3.2. Base case

A successful ignition and complete combustion of the sample is defined when most (> 95%) of the organic matter is consumed, and only a small amount of char remains due to extinction near the deep boundary. If ignition succeeds, simulations show that the following spread in the 40 mm deep samples lasts for about 1 h, similar to the observed average spread rate of 30 mm/h in [6]. Computational results show that the spread rate decreases with MC.

Arbitrarily, we choose a base case (SC sample, MC = 30% and IC = 40%) to investigate the combustion process in detail. Figure 2 shows the evolution of temperature profile. Right after ignition (3 min), the smoldering front reaches the peak temperature (~ 900 °C), and then spreads downwards along with the free surface regression. In the middle of the sample ($10 < z < 30$ mm, $t < 25$ min), where drying and peat-decomposition stages are important, the peak temperature stabilizes at about 650 °C, agreeing with the experimental observation in [5]. Near the deep boundary, char-oxidation dominates and the peak temperature increases upon 800 °C. Combustion is quenched at the deep end due to heat loss and the lack of peat.

Figure 3a shows that water is vaporized within 20 min; peat is decomposed within 27 min; and char-oxidation dominates the rest of time. Figure 3b shows that the peak mass-loss rate occurs at the beginning of ignition heating, along with a quick regression of the fuel bed. Once the ignition source is removed, the mass-loss rate suddenly drops, and then slowly decreases during the peat-decomposition stage. The fuel bed continues to shrink rapidly due to both the mass loss and the density increase from peat to char. When the char-oxidation dominates, the mass-loss rate slightly decreases due to both the end heat loss and the limited oxygen supply with the accumulation of mineral residue. The regression becomes slower

because the mass loss is compensated by the density decrease from char to ash.

Figure 3c shows the spread at $t = 15$ min. At this instant, the thickness of smoldering front is about 25 mm, and there are three sub-fronts (from deep to shallow): drying, peat decomposition, and char oxidation, and their reaction rates are on the same order of magnitude. The reaction rate of peat oxidation is two orders of magnitude smaller than peat pyrolysis (too small to be observed in Fig. 3c) because most of the oxygen is consumed in the char-oxidation sub-front and little oxygen diffuses through the deeper peat-decomposition sub-front. Consequently, very little of β-char is generated, and the β-char oxidation is small, agreeing with the previous prediction using a simplified plug-flow model [12]. Near the end of smoldering, only char is left, and the char-oxidation rate is high, thus increasing the temperatures in this region (see Fig. 2).

4. Smoldering thresholds

The MC_c measured in experiments of modified samples is plotted against IC_c in Fig. 4, and fitted by a linear correlation, $MC_c = 1.1 - 1.35 IC_c$ as in [6]. The experimental data of natural samples in [7] is also plotted. In general, Frandsen's linear correlation provides a reasonable reference for smoldering thresholds, but experimental data shows that some soil samples can still burn some distance above the line. This is probably due to the differences in decomposition kinetics, ignition protocol, and physical properties. The influences of these factors are investigated here using the 1-D model.

4.1. Influence of kinetic parameters

By fixing IC_c over a range of values, MC_c can be found by increasing the moisture until the incomplete combustion occurs. On top of the SC peat, the smoldering threshold for another three peat types from Siberia (SI-A and SI-B) and China (CH) were also computed with the corresponding kinetic parameters found in [12]. The SI-A peat also has a high organic content (IC = 2.4%), so the critical curve similar to that of SC peat is obtained. For the high-mineral samples of SI-B and CH peat (natural IC = 12.1% and 18.7%), only one critical point, MC_c(natural IC), is included in Fig. 4.

Figure 4 shows that the computed critical curve for both SC and SI-A samples are nonlinear. For SC peat, the critical curve crosses the middle of the experimental data scatter. The critical curve of SI-A samples is much lower, i.e. requires a much lower MC to ignite. The MC_c of SI-B and CH samples falls above and below the curve for SC. In short, the decomposition
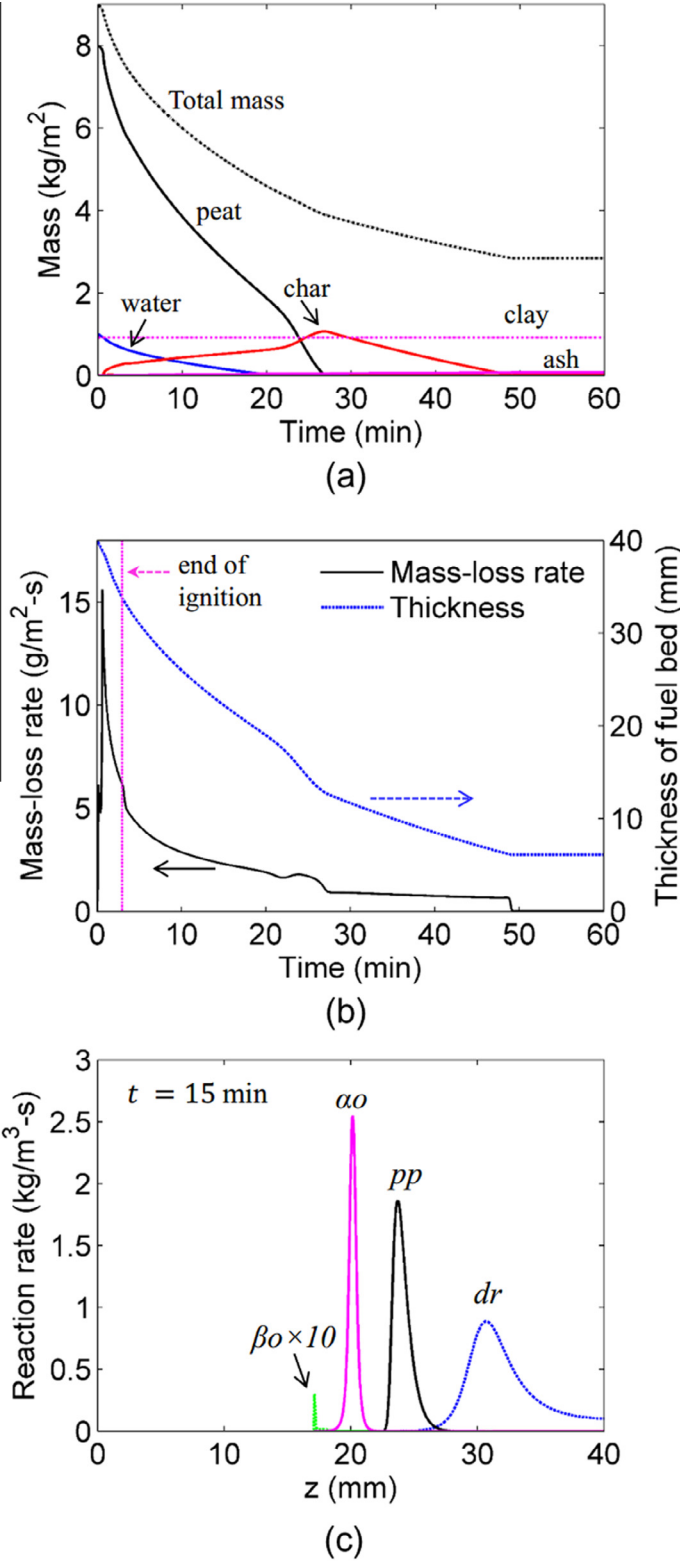
Fig. 3. Predicted evolution of (a) mass of each species condensed species, (b) total mass-loss rate and thickness of fuel bed, and (c) reaction-rate profile at t = 15 min for SC peat with MC = 30% and IC = 40%.
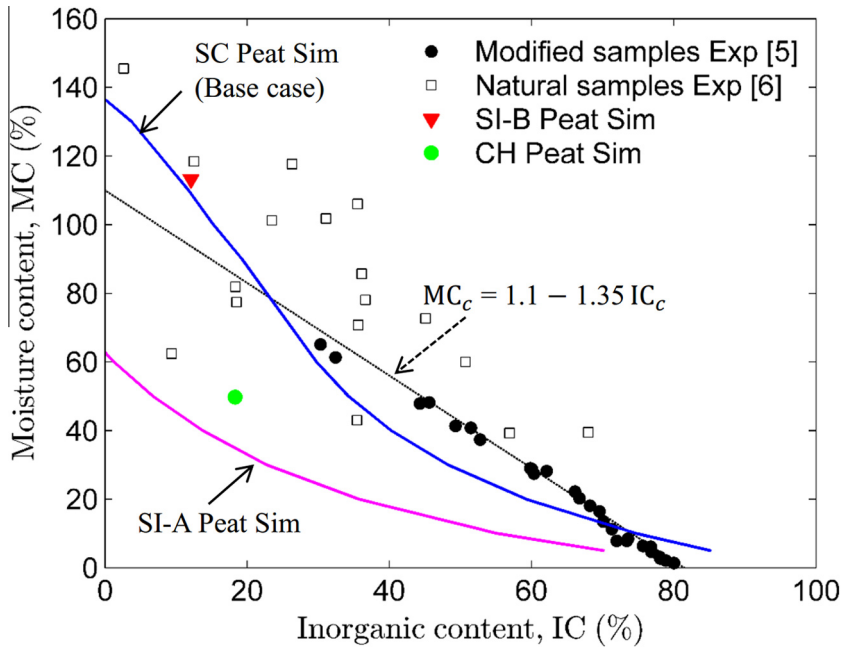
Fig. 4. Predicted and measured critical curves MC_c vs. IC_c for the smoldering ignition thresholds of different soils. Above the curve, a soil sample cannot ignite.
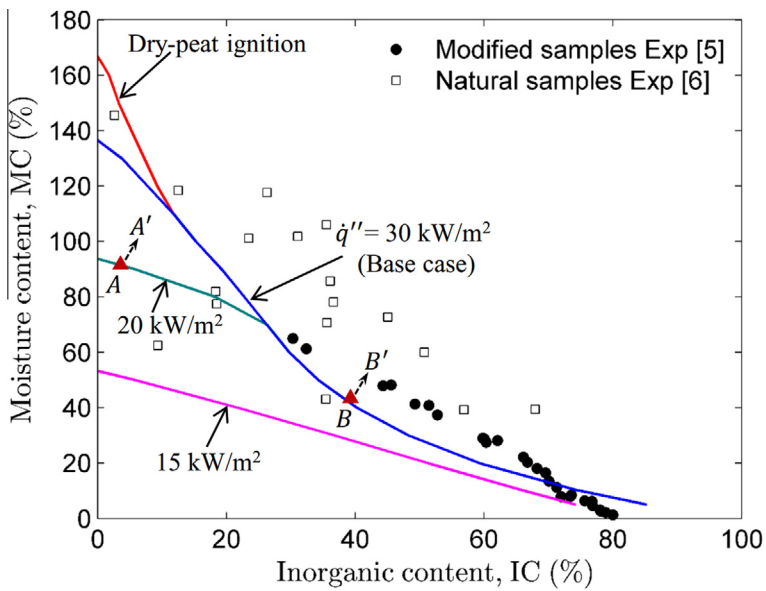

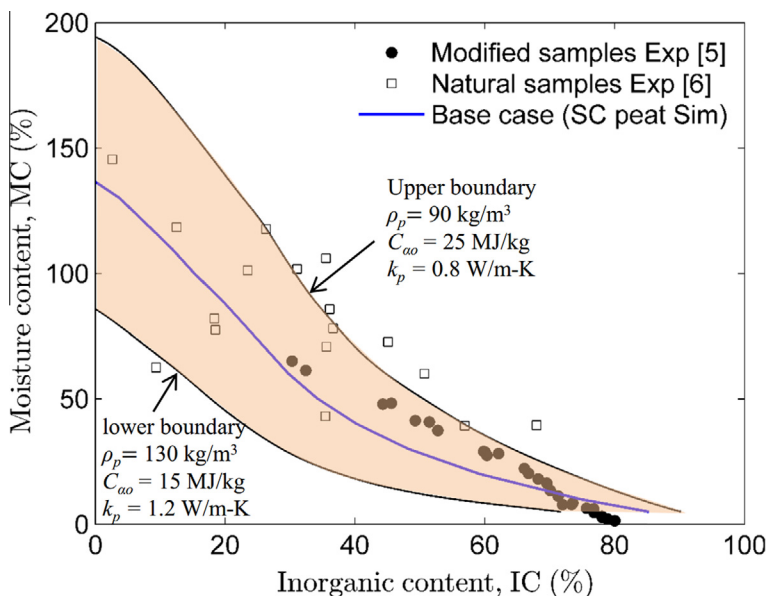Fig. 5. Predicted smoldering thresholds with different ignition protocols.

Fig. 6. Predicted smoldering thresholds for a combination of ρ_p, $k_{s,p}$, and $C_{\alpha o}$, varying in a wide range.

kinetics have a significant influence on smoldering thresholds.

4.2. Influence of ignition protocol

The influence of ignition protocol on the smoldering thresholds is investigated by varying the external heat flux in the range from 15 to 30 kW/m². The results are shown in Fig. 5. The minimum heat flux to ignite a dry SC peat, whose MC is in equilibrium with the ambient ($MC_{dr} \simeq 10\%$ [17,18]), is found to be 10.5 kW/m² for 3 min of heat, and 5.8 kW/m² for 30 min. This critical heat flux is much lower than the typical value for flaming fires (~30 kW/m²) [21]. The dry-peat ignition protocol used in the second set of experiments of [7] is also simulated by adding 1 cm of dry peat on the top which is heated for the same 3 min under 30 kW/m².

For organic soils with IC < 30%, increasing the heat flux extends the smoldering threshold because the drying of the whole sample bed induced by the ignition source increases. Slightly above the critical curve (e.g. point $A \rightarrow A'$), the reaction zone is quickly quenched (<5 min) near the top surface within the preheated zone. Therefore, for these cases, the threshold is defined as the critical moisture of ignition ($MC_{c,ig}$). For mineral soils with IC > 30%, the influence of the ignition protocol becomes negligible. Slightly beyond the critical curve (e.g. $B \rightarrow B'$), the smoldering front is able to spread out of the preheated zone for a distance before extinction. These cases were recorded as "partial burn" in the experiments of [6,7], therefore, the threshold is defined as the critical moisture of extinction ($MC_{c,ig}$).

The results show that the dry-peat ignition protocol is nearly equivalent to a heat flux of 55 kW/m² without the additional layer of dry peat. Once ignited, a sustained smoldering front is generated so that the threshold is for extinction. When the heat flux is very low (~15 kW/m²), the whole critical curve declines, and the threshold is for ignition.

4.3. Sensitivity to properties and heat of combustion

The physical properties of peat are expected to vary somehow for different ecosystems. This might affect the smoldering thresholds. Here, the sensitivity of the thresholds is investigated with combinations of the three most important parameters varying over wide ranges of values found in the literature: bulk density of peat (ρ_p = 90–130 kg/m³ [6]), solid thermal conductivity of peat ($k_{s,p}$ = 0.8–1.2 W/m K [13]), and heat of char oxidation ($C_{\alpha o} = C_{\beta o}$ = 15–25 MJ/kg [17]). Figure 6 reveals that the range of predicted smoldering thresholds covers most of the experimental data.

Computational results show that MC_c increases monotonously with the heat of combustion, but decreases with the bulk density and the thermal conductivity. Therefore, the case with maximum $C_{\alpha o}$ and minimum ρ_p and $k_{s,p}$ gives the upper boundary (see Fig. 6). As $C_{\alpha o}$ increases, the heat-generation rate increases, overcoming the heat-sink effect of water and minerals. The increase in $k_{s,p}$ is almost equivalent to the increase

in IC regarding the threshold, thus lowering the critical curve (i.e. more difficult to smolder), especially at low IC values. As ρ_p increases, the mass concentrations of water and clay also increase under the same MC and IC. Therefore, the increasing heat-sink effect moves the critical curve towards lower MC values, agreeing with experimental observations in [22].

5. Conclusions

In this work, a comprehensive 1-D model of a reactive porous media is implemented in the open-source code Gpyro to investigate the smoldering combustion of peat with a 5-step (including drying) heterogeneous kinetics. Two sets of small-scale experiments [7,6] are simulated for the first time, and the transient temperature, species, reaction profiles, and surface regression of the fire are studied. The predicted smoldering thresholds related to the critical moisture and inorganic contents are nonlinear, as opposed to previously reported linear correlation, and show a better agreement with the experimental results for a wide range of soil types. The smoldering thresholds are found to depend on the decomposition kinetics, physical properties, and the ignition protocol. The results reveal that the threshold values found by Frandsen for organic soils are due to ignition, and for mineral soils are due to extinction. This is the first time that a physics-based model of smoldering peat fires is developed, thus helping to understand this important natural and widespread phenomenon.

Acknowledgements

References

[1] T. Ohlemiller, *Prog. Energy Combust. Sci.* 11 (1985) 277–310.
[2] G. Rein, in: C. Belcher (Ed.), *Fire Phenomena and the Earth System*, Wiley and Sons, 2013, pp. 15–33.
[3] S.E. Page, F. Siegert, J.O. Rieley, H.-D.V. Boehm, A. Jaya, S. Limin, *Nature* 420 (2002) 61–65.
[4] L. Moreno, M.-E. Jimenez, H. Aguilera, P. Jimenez, A. Losa, *Fire Technol.* 47 (2011) 519–538.
[5] G. Rein, N. Cleaver, C. Ashton, P. Pironi, J.L. Torero, *Catena* 74 (2008) 304–309.
[6] W.H. Frandsen, *Can. J. Forest Res.* 17 (1987) 1540–1544.
[7] W.H. Frandsen, *Can. J. Forest Res.* 27 (1997) 1471–1477.
[8] G. Rein, A.C. Fernandez-Pello, D.L. Urban, *Proc. Combust. Inst.* 31 (2007) 2677–2684.
[9] C. Di Blasi, *Combust. Sci. Technol.* 106 (1995) 103–124.
[10] F. He, N. Zobel, W. Zha, F. Behrendt, *Biomass Bioenergy* 33 (2009) 1019–1029.
[11] C. Lautenberger, C. Fernandez-Pello, *Fire Safety J.* 44 (2009) 819–839.
[12] X. Huang, G. Rein, *Combust. Flame* 161 (2014) 1633–1644.
[13] R. Jacobsen, E. Lemmon, S. Penoncello, Z. Shan, N. Wright, in: A. Bejan, A. Kraus (Eds.), *Heat Transfer Handbook*, John Wiley & Sons, 2003, pp. 43–159.
[14] H. de Jonge, M.C. Mittelmeijer-Hazeleger, *Environ. Sci. Technol.* 30 (1996) 408–413.
[15] B. Punmia, A. Jain, *Soil Mechanics and Foundations*, Laxmi Publications Pvt Limited, 2005.
[16] R.M. Hadden, G. Rein, C.M. Belcher, *Proc. Combust. Inst.* 34 (2013) 2547–2553.
[17] K. Bergner, C. Albano, *Anal. Chem.* 65 (1993) 204–208.
[18] H. Chen, W. Zhao, N. Liu, *Energy & Fuels* 25 (2011) 797–803.
[19] W.H. Frandsen, *Int. J. Wildland Fire* 1 (1991) 197–204.
[20] C. Huggett, *Fire Mater.* 4 (1980) 61–65.
[21] D. Drysdale, *An Introduction to Fire Dynamics*, Wiley, 2011.
[22] R. Hartford, *Proc. 10th Conf. Fire Forest Meteorol.* (1989) 282–286.